



# Distribution of zooplankton biomass and potential metabolic activities across the northern Benguela upwelling system



I. Fernández-Urruzola<sup>a,\*</sup>, N. Osma<sup>a</sup>, T.T. Packard<sup>a</sup>, M. Gómez<sup>a</sup>, L. Postel<sup>b</sup>

<sup>a</sup> Plankton Ecophysiology Group, Instituto de Oceanografía y Cambio Global, Universidad de Las Palmas de Gran Canaria, 35017 Canary Islands, Spain

<sup>b</sup> Zooplankton Ecology Group, Baltic Sea Research Institute, D-18119 Rostock, Warnemünde, Germany

## ARTICLE INFO

### Article history:

Received 26 August 2013

Received in revised form 14 May 2014

Accepted 16 May 2014

Available online 24 May 2014

### Keywords:

Zooplankton

Biomass

Electron transport system (ETS)

Glutamate dehydrogenase (GDH)

Benguela upwelling system

## ABSTRACT

The distribution of zooplankton biomass and potential metabolic rates, in terms of electron transport system (ETS) and glutamate dehydrogenase (GDH), were analyzed along a cross-shelf transect in waters off Namibia. The highly variable dynamics of upwelling filaments promoted short-term fluctuations in the zooplankton biomass and metabolism. Maximum values were characteristically found over the shelf-break, where zooplankton biomass as dry mass (DM) reached peaks of  $64.5 \text{ mg m}^{-3}$  within the upper 200 m in late August. Two weeks later, the zooplankton-DM decreased by more than a third ( $19 \text{ mg DM m}^{-3}$ ). Zooplankton potential respiration and  $\text{NH}_4^+$  excretion averaged  $234 \mu\text{mol O}_2 \text{ m}^{-3} \text{ d}^{-1}$  and  $169 \mu\text{mol NH}_4^+ \text{ m}^{-3} \text{ d}^{-1}$  in the Namibian shelf, respectively. High protein-specific ETS activities even in the low-chlorophyll waters outside the filament suggested a shift into greater omnivory seaward. In this light, zooplankton elemental and isotopic compositions were used to investigate the pelagic food web interactions. They evidenced spatial changes in the carbon resource for zooplankton as well as changes in the form of nitrogen that fueled the biological production in aging advected waters. Overall, both aspects of zooplankton metabolism impacted the primary productivity at a level less than 10% under all the different oceanographic conditions.

© 2014 Elsevier B.V. All rights reserved.

## 1. Introduction

Upwelling ecosystems are among the most productive areas in the ocean. They mainly occur along the eastern boundaries of an ocean where the wind-driven divergence forces deep cold waters, rich in nutrients, into the sunlit layer. Both nutrient enrichment and light availability together, provide a suitable environment for sustaining high biological productivity. One of the major eastern boundary current systems of the world is the Benguela, which is divided in two sub-systems by a permanent upwelling cell located around  $27\text{--}28^\circ\text{S}$  (Boyer et al., 2000). Here, the northern part is the focus of investigation. It is limited by the warm water of the Angola–Benguela Front (Shannon, 2001) and exhibits important instabilities at short temporal and spatial scales in addition to the well-documented interannual fluctuations (Hutchings et al., 2009; Shannon and Nelson, 1996). Both oceanographic and atmospheric forces intensify the upwelling pulses during the austral winter and spring, and relax them in autumn (Boyd et al., 1987). Other processes such as jets and filaments emerging from the perennial cell also promote the variability in the northern Benguela ecosystem. These mesoscale structures will ultimately impact the plankton populations dynamics.

In this and in all upwelling systems, mesozooplankton play a key role in the mass and energy flows through the food web (Moloney, 1992). They are the primary food resource for fish larvae and consequently, the main trophic link to the top predators. In recognizing the importance of zooplankton in the Benguela system, several studies have paid attention to its spatial distribution (Hansen et al., 2005; Olivar and Barangé, 1990; Postel et al., 2007; Verheye and Hutchings, 1988, among others), as well as to the long-term trends in the zooplankton abundance (Verheye et al., 1998) and biomass (Huggett et al., 2009). Changes in the community composition (Gibbons and Hutchings, 1996; Verheye et al., 2001), ecology (Gibbons et al., 1992; Verheye et al., 1992) and secondary production (Hutchings et al., 1991; Richardson and Verheye, 1999) in relation to physical and biological forcings have also been described in the last decades. However, these studies have not considered the short-term zooplankton structural dynamics caused by successive upwelling-relaxation events, filaments or eddies which take place in a particular region. Wind-driven offshore advection, for instance, causes the stratified plankton-rich waters to be rapidly replaced by deeper waters, which introduce a new batch of nutrients into the photic layer, but little plankton. Accordingly, the inherent variability of these chemical and physical phenomena constrains the integrity of biological communities on the order of days.

Furthermore, the instability of the oceanographic setting also affects the physiological dynamics of zooplankton (Gaudy and Youssara, 2003). Respiration and  $\text{NH}_4^+$  excretion are important processes in marine

\* Corresponding author. Tel.: +34 928 45 44 73; fax: +34 928 45 29 22.  
E-mail address: [ifernandez@becarios.ulpgc.es](mailto:ifernandez@becarios.ulpgc.es) (I. Fernández-Urruzola).

ecology, as the balance between synthesis and demand of both carbon and nitrogen controls the efficiency of the net production (Margalef, 1982). In this context, Chapman et al. (1994) measured electron transport system (ETS) activities in microplankton to broadly estimate the carbon requirements and the nutrient regeneration in the waters south of Walvis Bay. Few studies have directly dealt, however, with mesozooplankton metabolism in this upwelling ecosystem. Recently, Huenerlage and Buchholz (2013) demonstrated variations in the physiological behavior of *Euphausia hansenii* under changeable trophic conditions in the Angola–Benguela frontal waters. The respiration in terms of ETS activity was also determined, but only on the dominant copepod species from Benguela (Bode et al., 2013; Timonin et al., 1992). Indeed, from respiration measurements, Schukat et al. (2013) assessed an important daily phytoplankton removal by copepods. Here we elucidate the magnitude of the respiration and  $\text{NH}_4^+$  excretion rates by the total mesozooplankton community in a cross-shelf transect off Namibia. We used the enzymatic approach because direct measurements of physiology such as the water-bottle procedures give low spatial resolution and are additionally complicated by artifacts derived from organism manipulation, overcrowding and even starvation when long incubation times are needed (Bidigare, 1983). Enzymatic assays in turn, require the addition of saturating levels of substrates to ensure the specificity of the reaction (Maldonado et al., 2012; Segel, 1993), resulting in a potential measurement which gives the maximum rate ( $V_{max}$ ) instead of the actual one. Nevertheless, studies have demonstrated the utility of enzymes as an accurate index of metabolic rates, specially when they are previously calibrated for the surveyed system (e.g., Bode et al., 2013; Hernández-León et al., 1999; Packard, 1985).

This field study is embedded in an interdisciplinary research of the aging process of a coastal upwelling system. We aimed to characterize how the physical structuring processes affect the biomass of zooplankton, as well as to describe the impact that zooplankton metabolism has on the primary productivity from the northern Namibian cell. Elemental composition and stable isotopes of zooplankton were additionally used to infer spatial changes in the pelagic food web of this ecosystem. Since continuous monitoring is required to understand the structure and functioning of the plankton community, we applied a

Eulerian approach by sampling a cross-shelf transect four times during a month of intense wind-forcing. The irruption of eddies and filaments will affect the maturation pattern of the fresh upwelled waters along its pathway seaward. This influences the successional developments in these aging advected waters, promoting the heterogeneity in zooplankton populations towards the open ocean. In this scenario, our research illustrates the dynamics of zooplankton biomass and potential metabolism in face of the different oceanographic situations recorded in the northern Benguela.

## 2. Material and methods

Four consecutive transects were made to collect zooplankton samples and hydrographic data at 20°S off Namibia during the SUCCESSION cruise onboard RV Maria S. Merian from August 27th to September 15th, 2011. Three of the transects sampled 12 stations to a distance of 230 km from the coast, while the fourth one was extended seaward by 9 stations to 500 km (Fig. 1). Stations from NAM001 to NAM018 were sampled during both day and night in order to minimize the effect of the vertical migrations by the large zooplankton. Salinity, temperature, chlorophyll-a fluorescence and dissolved oxygen profiles were obtained at each station by deployment of a CTD SBE 911+, equipped with a WETlab FLRT-1754 fluorometer, and mounted on a rosette sampler with twenty-four 10 L Niskin bottles. Nutrients ( $\text{NO}_2^-$ ,  $\text{NO}_3^-$ ,  $\text{PO}_4^-$ ,  $\text{NH}_4^+$  and  $\text{SiO}_4^{4-}$ ) as well as chlorophyll-a concentrations were also measured at different depths (Mohrholz et al., 2014; Nausch and Nausch, 2014).

### 2.1. Zooplankton sampling

Zooplankton was collected by Multinet vertical hauls (Hydrobios GmbH, Kiel, Germany). The equipment consisted of a net frame with an opening of 0.25 m<sup>2</sup>, fitted alternatively with 100 and 500 μm meshed nets (L = 2.5 m, diameter at the end = 0.11 m) and stabilized by V-fin depressor. Each net ended in a cod-end consisting of a plastic bucket with side windows covered by gauze. The two flowmeters, mounted inside and outside of the frame, measured the amount of water filtered by

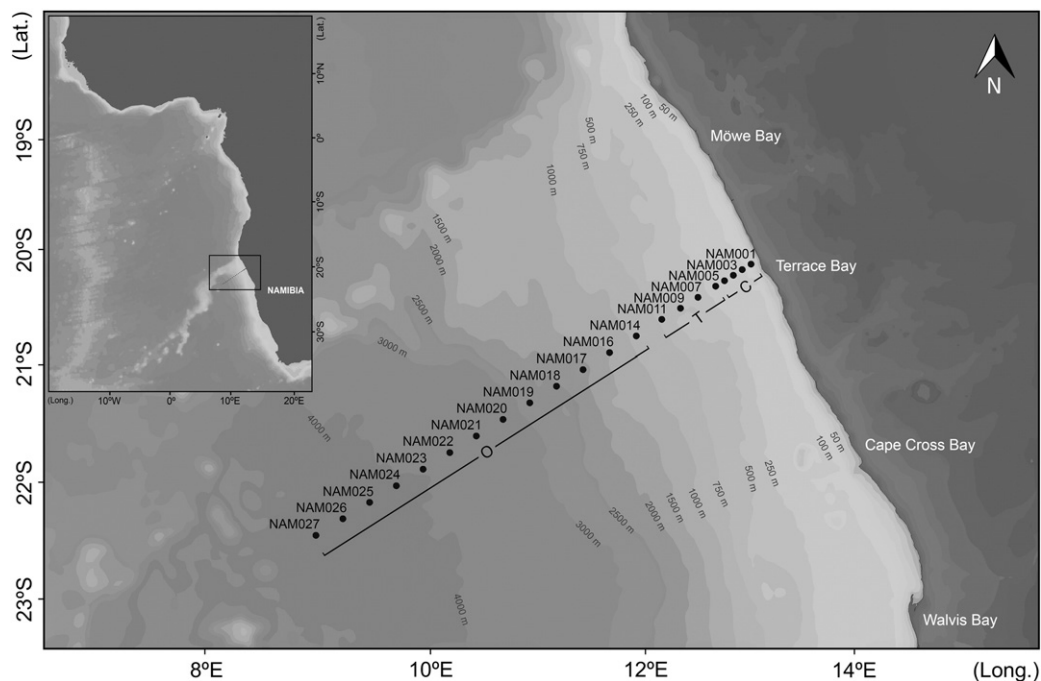


**Fig. 1.** Map of the study area showing the cross-shelf transect of the Namibian upwelling where zooplankton samples were collected during the SUCCESSION cruise. Stations from NAM001 to NAM018 were sampled four times, while samples from NAM019 to NAM027 were collected only once. The transect was divided into coastal (C), transition (T) and offshore (O) areas according to the geological and oceanographical properties of the stations.

the net during each haul, and a pressure sensor recorded the depth in real-time. The multiple open/closing system enabled the collection of stratified zooplankton samples in a single deployment. Three depth layers were sampled: from 200 to 75 m (or 10 m from the bottom in the shallower stations), 75 to 25 m and 25 m to the sea surface. Net sets with the two mesh sizes sampled each strata, so two samples per depth layer were recovered. We used the 100  $\mu\text{m}$  mesh size for the zooplankton fractions below 500  $\mu\text{m}$ , and the 500  $\mu\text{m}$  mesh size for the larger ones. This approach ensured a quantitative sampling for size fractions below 10 mm.

Once on deck, the net was rinsed with seawater and the samples were maintained at 4 °C while awaiting the processing. First, we split the samples by the beaker technique (Van Guelpen et al., 1982). One half was fractionated for the 100–200, 200–500, 500–1000 and >1000  $\mu\text{m}$  size classes, and immediately frozen in liquid nitrogen before being stored in the freezer (–80 °C) for subsequent enzymatic analyses. The other was split into two new subsamples: one was frozen at –20 °C for biomass and isotopic determinations; the other was stored in plastic bottles filled with buffered formaldehyde (4% final concentration) for taxonomic analysis. Size fractionation was made in both cases as well. Organisms over 5000  $\mu\text{m}$  such as jellyfish were not included in our calculations. However, they were counted and the diameter of the umbrella was measured with a calibrated rule in order to convert them into dry mass (DM) using the equation  $\text{DM} = 0.03 \text{ Diameter}^{2.3}$  given in Møller and Riisgård (2007) for the genus *Aquarea*.

Chains of diatoms were found in a few 100  $\mu\text{m}$  meshed net hauls in the surface layer from NAM005 to NAM009, mainly during the first two transects. Despite the samples being carefully washed with filtered seawater, some diatoms still remained in them. This contamination was noticeable in only 18% of the samples. In order to quantify the biomass due to phytoplankton in these samples, the amount of chlorophyll-*a* was first determined by spectrophotometry (Parsons et al., 1984). Then, chlorophyll-*a* values were converted into organic carbon with a factor of 27 ( $\mu\text{g C}/\mu\text{g chl-a}$ ) calculated from the relationship:  $C = 24.3 \text{ chl-a} + 29.3$  ( $n = 29$ ,  $r^2 = 0.75$ ,  $p < 0.05$ ) given in Schlüter and Havskum (1997) with the intercept forced through zero. This factor agrees with others reported for marine phytoplankton communities in an exponential growth phase (Banse, 1977; Smetacek and Hendrikson, 1979). For communities in senescence with high detrital presence, the relationship between carbon and chlorophyll-*a* can rise up to 200. This was not the case here. Since the samples in question were found in mature waters rich in nutrients, suitable for a bloom of diatoms, the lower limit of the C/Chl-*a* ratio (ranging from 22 to 200) was used. Accordingly, these should be considered as conservative estimates. The phytoplankton-associated carbon value was subtracted from the total organic carbon of each contaminated sample. On average, these zooplankton samples contained  $35 \pm 24\%$  phytoplankton biomass. Afterwards, our own ratios (see Results) were applied to Ricker's concept based on the sum of the least products (Ricker, 1973) so as to recalculate the biomass of zooplankton in terms of DM, organic nitrogen and protein in these samples.

## 2.2. Biomass analyses and stable isotopes measurements

Frozen samples were dried at 60 °C in the land-based laboratory. The isotope, particulate organic carbon (POC) and particulate organic nitrogen (PON) samples were ground to fine powder and weighed in tin capsules. Measurements were made by means of Flash combustion in a CE Instruments Flash EA 1112 at 1020 °C in a Finnigan Delta S isotope ratio mass-spectrometer via a Conflow III open split interface. Calibration for the total POC and PON determinations was done daily with anacetanilide standard. The stable nitrogen and carbon isotope ratios measured for each sample were corrected with the values obtained from standards with defined nitrogen and carbon element and isotopic compositions (International Atomic Energy Agency IAEA: IAEA-N1, IAEA-N2, IAEA-N3, NBS 22, IAEA-C3 and IAEA-CH-6) by mass balance. Values are reported

relative to atmospheric  $\text{N}_2$  ( $^{15}\text{N}$ ) and VPDB ( $^{13}\text{C}$  – Vienna Pee Dee belemnite). The analytical precision for both stable isotope ratios was 0.2%. Carbon and nitrogen contents were calculated by the percentages of the initial dry masses in relation to the total. Then, considering the split part and the amount of water filtered, the carbon and nitrogen concentrations were given in  $\text{mg m}^{-3}$ . C/N ratios were calculated on a molar basis. Samples were not generally acidified prior to combustion in order to remove inorganic carbon. An experiment using 45 samples selected by chance served as a data base to estimate the effect. The average of non acidified samples amounted to  $25.1 \pm 6.9\%$  as compared to  $22.4 \pm 7.1\%$  after acidifying them. The difference amounted to a maximum of 7.5%, but was not significant ( $p > 0.05$ ). None of the zooplankton samples contaminated with phytoplankton were considered for isotope characterization. In addition, biomass in terms of protein content was determined from the samples kept for enzyme activities by using the method of Lowry et al. (1951) modified by Rutter (1967).

## 2.3. Zooplankton community composition

Taxonomic analysis was done with great deliberation on all size classes and all depth levels down to 200 m from five transect II stations. The distance to shore was 10, 20, 110, 200, and 230 km or a “pseudo-age” (Mohrholz et al., 2014) of 4.0, 3.7, 48.9, 46.4 and 44.5 days, respectively. Transect II was chosen to facilitate a later comparison with the results obtained by the Video-Plankton-Recorder VPR II, which produces the same taxonomic resolution, but at higher sampling frequency. Samples were taken at night except for NAM001, which was taken at dawn. As a result, the vertical profiles were not affected by daily vertical migration and consequently, are comparable.

The species analysis of the larger zooplankton required a stereomicroscope (Leica, MZ 8) with a magnification between 16 and 80 $\times$ . The smaller size classes were analyzed by an inverted microscope (Labovert FS, Leitz) usually with a magnification of 50 $\times$ . In both cases, Bogorov trays of suitable sizes were used for counting. The total samples were first surveyed for rare specimens. High sample concentrations often required the analysis of sub-samples. The entire procedure and the discussion of errors have been described in detail in Postel et al. (2000). Taxonomic determinations were performed to different levels, often down to genera, using the literature for the Angolan–South African region (Gibbons, 1997), the South Atlantic (Boltovskoy, 1999), the northern hemisphere (ICES, 2001) and the Mediterranean (Riedl, 1983; Trégouboff and Rose, 1978).

## 2.4. Indices of metabolism

Electron transport system (ETS) and glutamate dehydrogenase (GDH) activities were measured on the same homogenate that was used for protein determination. During the whole procedure, the samples were kept in ice in order to prevent a decline in the enzymatic activities. The supernatant fluid was assayed for ETS activity following the Owens and King (1975) methodology, and for GDH activity using the procedure of Bidigare and King (1981) modified according to Fernández-Urruzola et al. (2011). Both analyses were carried out kinetically at 18 °C and then corrected for temperature. This recalculation assured an accurate estimation of the in situ respiration and  $\text{NH}_4^+$  excretion by employing the Arrhenius equation with activation energies of 15  $\text{kcal mol}^{-1}$  (Packard et al., 1975) and 10  $\text{kcal mol}^{-1}$  (calculated from Park et al., 1986), respectively. The phytoplankton associated-ETS activities in the aforementioned samples were subtracted from the total ETS by means of an ETS to zooplankton–protein ratio equal to 61.6  $\mu\text{mol O}_2 \text{ mg protein}^{-1} \text{ d}^{-1}$ . This factor was obtained by regression analysis of non-contaminated zooplankton smaller than 500  $\mu\text{m}$ , and sampled from the same area (ETS activity = 61.6 protein,  $n = 91$ ,  $r^2 = 0.93$ ,  $p < 0.001$ ). However, it was not necessary to correct the GDH activities since the deamination function for  $\text{NAD}^+$ -specific GDH in phytoplankton is negligible (King, 1984; Park et al., 1986).



Additionally, water-bottle incubations for respiration and  $\text{NH}_4^+$  excretion were conducted on board in order to calibrate the enzymatic measurements with specific R/ETS and GDH/ $\text{NH}_4^+$  ratios for the Benguela system. Zooplankters were collected by WP-2 net hauls and after fractionation, maintained in filtered seawater at sea surface temperature (14–16 °C). After an hour acclimation period, the healthiest organisms were incubated in filtered seawater at 14 °C for 2 h in glass-capped bottles. All the experiments included at least one control flask. Oxygen consumption was estimated by the continuous measurement of dissolved  $\text{O}_2$  with a 6-channel Strathkelvin 928 Oxygen System® respirometer. Once the incubation was finished, a sample of seawater (10 ml) was siphoned off from each bottle for  $\text{NH}_4^+$  determinations in accordance with the phenol-hypochlorite method (Solorzano, 1969). Afterwards, the zooplankters were removed and frozen at  $-80$  °C in order to analyze the enzyme activities as described above. The mean R/ETS value for zooplankton was  $0.48 \pm 0.29$  ( $n = 19$ ), while for GDH/ $\text{NH}_4^+$  it was  $16.4 \pm 12.2$  ( $n = 26$ ). Although the standard deviations were high, these ratios are close to the reported R/ETS ratio by Bode et al. (2013) for the same region, and in the middle of the range of GDH/ $\text{NH}_4^+$  ratios from the literature (Fernández-Urruzola et al., 2011). The errors caused by these ratios have been discussed by King and Packard (1975), and Hernández-León and Gómez (1996). Furthermore, del Giorgio (1992) found that these errors were not greater than those of other methods used in standard ecological procedures for plankton metabolic processes, such as the thymidine and  $^{14}\text{C}$  uptake techniques (Richardson, 1991). As a result, the average ratios measured here were used to estimate the community respiration and  $\text{NH}_4^+$  excretion throughout this study. Oxygen consumption rates were converted into carbon from the respiratory quotient of 0.86, assuming a mixed diet (Omori and Ikeda, 1984). The C/N uptake ratio of 6.1 ( $\mu\text{g C}/\mu\text{g N}$ ) given by Dugdale and Goering (1967) was used to assess the carbon regenerated by the zooplankton  $\text{NH}_4^+$  excretion rates. Gross primary production (GPP) was estimated from chlorophyll-a and  $^{14}\text{C}$  uptake measurements made on board; the calculations followed the procedure described in Brown et al. (1991) for the Benguela system, with the regression model (best fit to the data):  $^{14}\text{C} = 3.75 \text{ chlorophyll-a}^{0.653}$  ( $n = 24$ ,  $r^2 = 0.60$ ,  $p < 0.001$ ). The difference between GPP and the daily phytoplankton respiration (assumed to be 10% of hourly production multiplied by night hours) equaled the net primary production (NPP).

### 3. Results

Mohrholz et al. (2014) describe in detail the hydrographic conditions during the SUCCESSION cruise. Different water masses were present in the study area, most of them with a northern origin. Additionally, a cold water filament was found extending offshore from the coastal upwelling center. This filament influenced the near-shore stations, while the ones over 140 km from the coast were mainly under the influence of warmer water masses, especially at the end of the cruise. The phytoplankton development was coupled with the presence of the cold water filament, reaching a maximum peak of chlorophyll-a at the beginning of September. Ekman divergence dominated near the coast, whereas curl-driven upwelling introduced nutrient-rich South Atlantic Central Waters (SACW) into the euphotic zone with a maximum vertical velocity of  $0.35 \text{ m d}^{-1}$  around the outer shelf. These differences in hydrology allowed us to distinguish three regions within the transect (Fig. 1). The coastal stations (NAM001–NAM004) were characterized by the Ekman transport that brings deep central waters to the surface with high vertical velocities. The transition zone (NAM005–NAM011) occurred over the shelf-break and was strongly influenced by both the filaments and the curl driven upwelling. The offshore stations over the continental slope (NAM014–NAM027) were mainly affected by warmer southern water masses (ESACW) and by the occasional occurrence of younger waters arising from the filaments. The selection of the limits of these regions was strengthened by a cluster

analysis of physical and chemical properties of the stations (diagram not shown).

#### 3.1. Zooplankton biomass and community structure

The pattern of water masses at 20°S promoted great temporal variability in zooplankton biomass along the transect (Fig. 2). Accordingly, peaks of zooplankton were found coinciding with maximum values of chlorophyll-a in late August. At that time, a nearly stable cold water filament sustained high primary productivity, even at the outer stations such as NAM017 (see Hansen et al., 2014). Afterwards, the filament was dispersed to the northwest, which led to a decrease in the chlorophyll-a concentration as well as a three-fold decrease in the zooplankton biomass. In order to reduce the impact of these mesoscale structures, the measurements of the four transects were averaged for some analyses.

Despite the fact that the zooplankton and more particularly the size fractions over 500  $\mu\text{m}$  showed higher biomass during the night (Fig. 3), the non-parametric Mann–Whitney  $U$  test did not reveal a significant day–night difference ( $p > 0.05$ ). This means that only a small percentage of the larger zooplankton migrated out of the upper 200 m during the day. Nonetheless, the schedule of the sample collection during the cruise minimized those vertical differences by sampling two days and two nights at each station and averaging results over time. Larger horizontal differences of the biomass were observed among the areas (one-way ANOVA,  $F_{2,48} = 20.22$ ,  $p < 0.001$ ). The DM-values averaged  $51 \text{ mg m}^{-3}$  in the upper 75 m of the transition zone, a value much higher than those measured at the other two zones (Table 1). The development of salp blooms in the mature waters from the transition area during the first half of the cruise resulted in high biomass deviations in the largest size class.

The total zooplankton biomass peaked at all three depth layers at 90 km from the coast (Fig. 4). The maximum mean value in the surface layer was  $81 \text{ mg DM m}^{-3}$ . This occurred slightly displaced offshore from the diatom bloom that was found at 70 km from the coast. Then, the zooplankton biomass diminished seaward down to  $3 \text{ mg DM m}^{-3}$ , although an unexpected peak in the upper 25 m was found 380 km from the shore owing to the high abundance in the largest size fraction. The highest densities of zooplankton were always found in the upper 25 m, where the chlorophyll-a concentration was about two-fold greater than the one measured from 25 to 75 m, and almost one order of magnitude greater in comparison with the deepest layer. In general, our zooplankton biomass results were of similar magnitude to those registered in 1979 along the same transect (Southwest Atlantic cruise, SWA; see details in Postel, 1995). However, peaks of zooplankton during our cruise were displaced inshore compared to the earlier expedition (Fig. 4). Throughout the entire transect, cyclopid copepods were the most abundant taxa within the size fractions below 500  $\mu\text{m}$  (Fig. 5a). At the inner stations, the relative abundance of meroplanktonic larvae (ophioplutei) was also high (30%). They decreased further offshore, while the presence of other groups such as calanoids, harpacticoids and tintinnids increased. In the larger zooplankton there appeared more variability in the dominant species (Fig. 5b). Thaliaceans predominated at the shelf-break and calanoids were more important inshore and offshore. Jellyfish were not considered here, although we noted their presence mainly confined to the inner shelf (Fig. 6).

#### 3.2. Body composition and stable isotopes in zooplankton

The relationship between organic carbon and DM varied from 0.11 to 0.33, while protein and DM were related by a factor of  $0.18 \pm 0.05$ . Nitrogen content averaged 36% of the protein (see Table 1). Furthermore, the resulting C/N atomic ratios of zooplankton ranged between 4.2 and 6.4 (Fig. 7), with the values being significantly higher in the transition area (one-way ANOVA,  $F_{2,210} = 11.16$ ,  $p < 0.0001$ ; post hoc Tukey's HSD,  $p < 0.0001$ ). Only the C/N ratios of the microzooplankton

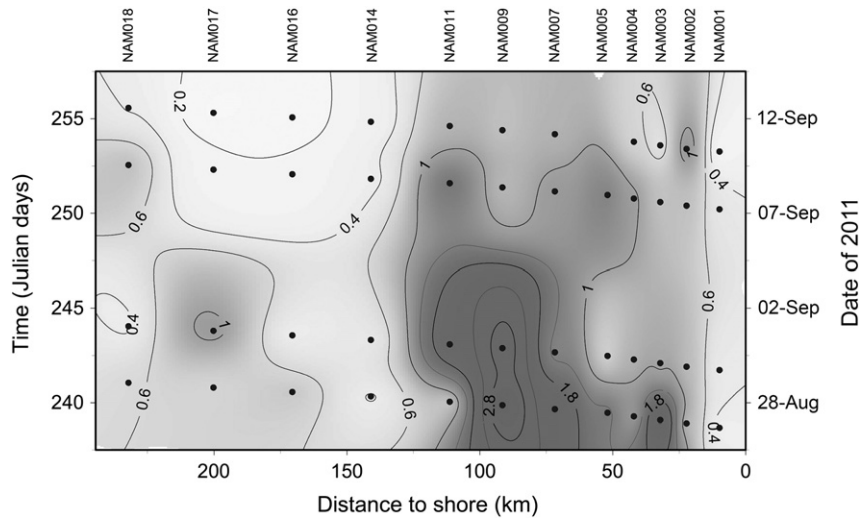


**Fig. 2.** Temporal variability of zooplankton biomass ( $\text{g DM m}^{-2}$ ) along the SUCCESSION transect. Only the first 25 m of the water-column is considered because this layer contains most of the variability. The secondary axis (right) shows the corresponding sampling-dates. Ocean Data View (ODV) software was used to generate interpolated values using the weighted averaged gridding method option.

(100–200  $\mu\text{m}$ ) were invariant throughout the transect (one-way ANOVA,  $F_{2,50} = 0.27$ ,  $p = 0.765$ ). Overall, the smaller size classes (100–200  $\mu\text{m}$  and 200–500  $\mu\text{m}$ ) tended to have C/N ratios above 5.2, whereas the larger size classes (500–1000  $\mu\text{m}$  and > 1000  $\mu\text{m}$ ) tended to have ratios below 5.2.

The averaged zooplankton- $\delta^{13}\text{C}$  (ranging from  $-21.3$  to  $-18.9\%$ ) revealed variability in the carbon source along the transect (Fig. 8). More negative  $\delta^{13}\text{C}$  values were mainly found in the inner stations (Kruskal–Wallis test,  $p < 0.005$ ). In the case of  $\delta^{15}\text{N}$ , the averaged zooplankton-values showed a more pronounced decrease from 11.0 to 4.8‰ within the first 100 km (Kruskal–Wallis test,  $p < 0.0001$ ). The individual patterns of the different size categories followed the same shape (data not shown). In addition, with increasing size, the zooplankton exhibited an enrichment in  $^{15}\text{N}$  and a depletion in  $^{13}\text{C}$ .

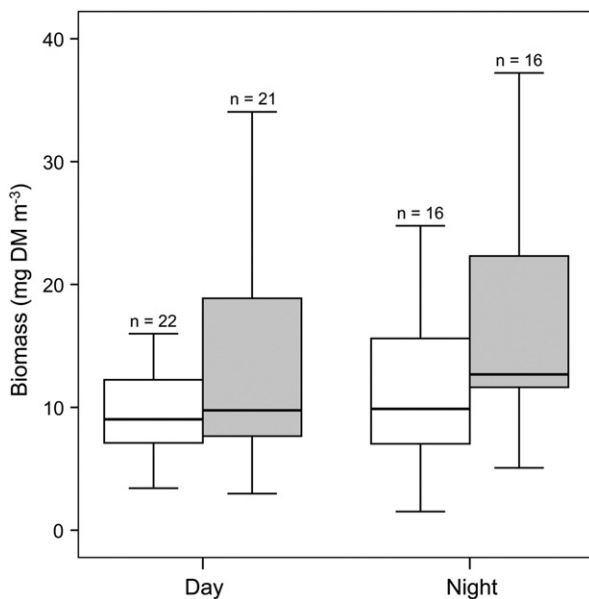


**Fig. 3.** Differences in zooplankton biomass distribution between day and night in the upper 75 m of the water-column. The gray boxes represent the zooplankton >500  $\mu\text{m}$  and the white boxes, the 100–500  $\mu\text{m}$  size fraction. The lower and upper boundaries of the boxes represent the first and third quartiles of the data distribution, respectively, with the dark line in the middle as the median. Error bars indicate the 95% confidence limits (C. L.).

### 3.3. Zooplankton metabolism

The zooplankton potential respiratory (ETS activity) and potential excretory (GDH activity) rates for the four transects are presented in Fig. 9. The highest metabolic activities were measured in late August (i.e., transects 1 and 2), which concurs with the pattern described for the zooplankton biomass. Thus, during the first two transects, the zooplankton enzyme activities exceeded by almost two-fold the ones measured in mid September (transect 4). A strong gradient in the ETS and GDH activities was also found with distance to shore. Highest metabolic rates were displaced further offshore by the filament during the transects 1 and 2. Accordingly, both enzyme activities peaked between NAM007 and NAM011. Afterwards, these peaks moved inward as the system became more stable and therefore, the zooplankton exhibited higher potential respiration and potential  $\text{NH}_4^+$  excretion rates from NAM002 to NAM005. Here in the upper 75 m, the averaged ETS activity was  $360 \pm 240 \mu\text{mol O}_2 \text{ m}^{-3} \text{ d}^{-1}$ , and the averaged GDH activity was  $320 \pm 155 \mu\text{mol NH}_4^+ \text{ m}^{-3} \text{ d}^{-1}$ . A second maximum appeared in the surface of NAM023 (transect 4) due to a patch particularly rich in large zooplankton, with values of  $490 \mu\text{mol O}_2 \text{ m}^{-3} \text{ d}^{-1}$  and  $316 \mu\text{mol NH}_4^+ \text{ m}^{-3} \text{ d}^{-1}$  for ETS and GDH, respectively (Fig. 9). The contribution of the smaller zooplankton (100–200  $\mu\text{m}$ ) to the total  $\text{NH}_4^+$  excretion was significantly greater in the near-shore stations (one-way ANOVA,  $F_{1,51} = 26.42$ ,  $p < 0.0001$ ). On the contrary, the high metabolic rates found in the transition waters were mainly associated with the largest size fraction.

Measurable differences in the protein-specific ETS activities were found when both region and size class were considered (one-way ANOVA,  $F_{11,196} = 8.53$ ,  $p < 0.001$ ). GDH activities per unit of biomass displayed similar variability (one-way ANOVA,  $F_{11,188} = 15.97$ ,  $p < 0.001$ ). In general, the zooplankton from the transition area had lower specific rates (Table 2). Here, the specific ETS activity of the largest size fraction dropped from 2.72 to 1.28  $\mu\text{mol O}_2 \text{ mg protein}^{-1} \text{ h}^{-1}$  (post hoc Tukey's HSD,  $p < 0.001$ ). This coincided with blooms of salps (Fig. 5b), which have a lower specific-metabolism. In contrast, the main decrease in the GDH activity was observed in the smaller size classes (100–200  $\mu\text{m}$  and 200–500  $\mu\text{m}$ ), as their rates declined by half to values of around 1.2  $\mu\text{mol NH}_4^+ \text{ mg protein}^{-1} \text{ h}^{-1}$  over the transition zone shelf-break (post hoc Tukey's HSD,  $p < 0.001$ ). The slopes of the regression of log-transformed data for both ETS and GDH scaled to exponents of 1.04 and 0.88 with protein mass, respectively (Fig. 10). These relationships showed positive correlations with a Pearson

**Table 1**

Cross-shelf distribution of averaged ( $\pm$ SD) zooplankton biomass for the three regions in terms of dry mass (DM), organic carbon (C), organic nitrogen (N) and protein (all in  $\text{mg m}^{-3}$ ) measured on four size fractions in the upper 75 m. The relative contribution (%) of each fraction to the total protein biomass is also given.

Area	Size ( $\mu\text{m}$ )	n	DM	C	N	Protein	%
Coastal	100–200	16	3.60 $\pm$ 1.54	1.08 $\pm$ 0.45	0.26 $\pm$ 0.11	0.63 $\pm$ 0.21	13.7
	200–500	16	6.61 $\pm$ 4.20	1.71 $\pm$ 0.94	0.46 $\pm$ 0.24	1.24 $\pm$ 0.60	27.1
	500–1000	16	3.50 $\pm$ 2.58	1.17 $\pm$ 0.89	0.33 $\pm$ 0.24	0.75 $\pm$ 0.54	16.3
	>1000	16	9.34 $\pm$ 8.94	2.89 $\pm$ 3.03	0.89 $\pm$ 0.85	1.97 $\pm$ 2.11	42.9
	Total	64	23.05 $\pm$ 10.32	6.85 $\pm$ 3.32	1.94 $\pm$ 0.92	4.59 $\pm$ 2.27	100
Transition	100–200	14	3.96 $\pm$ 3.00	0.67 $\pm$ 0.41	0.16 $\pm$ 0.09	0.67 $\pm$ 0.50	6.4
	200–500	14	16.44 $\pm$ 12.32	2.60 $\pm$ 1.71	0.57 $\pm$ 0.38	3.74 $\pm$ 3.12	35.8
	500–1000	16	4.12 $\pm$ 2.77	1.36 $\pm$ 0.94	0.36 $\pm$ 0.25	1.28 $\pm$ 1.02	12.3
	>1000	14	26.38 $\pm$ 34.18	7.01 $\pm$ 5.04	1.71 $\pm$ 1.16	4.75 $\pm$ 3.29	45.5
	Total	58	50.90 $\pm$ 36.56	11.64 $\pm$ 5.42	2.80 $\pm$ 1.24	10.44 $\pm$ 4.67	100
Offshore	100–200	23	1.87 $\pm$ 1.44	0.41 $\pm$ 0.29	0.10 $\pm$ 0.07	0.29 $\pm$ 0.18	10.4
	200–500	24	4.86 $\pm$ 4.58	1.03 $\pm$ 0.80	0.26 $\pm$ 0.20	0.68 $\pm$ 0.58	24.3
	500–1000	23	2.64 $\pm$ 1.82	0.84 $\pm$ 0.61	0.24 $\pm$ 0.18	0.47 $\pm$ 0.34	16.8
	>1000	24	8.51 $\pm$ 5.32	2.07 $\pm$ 1.39	0.57 $\pm$ 0.39	1.36 $\pm$ 1.14	48.6
	Total	92	17.88 $\pm$ 7.39	4.35 $\pm$ 1.74	1.17 $\pm$ 0.48	2.80 $\pm$ 1.34	100

coefficient of 0.92 for ETS and a non-parametric Spearman coefficient of 0.81 for GDH (in both cases,  $p < 0.0001$ ).

Estimations of the physiological rates of the zooplankton community reflected higher respiration and  $\text{NH}_4^+$  excretion at those stations where the primary productivity attained its maximum values (Table 3), with the largest size class contributing most (data not shown). However, the phytoplankton carbon which was respired in the upper 75 m by mesozooplankton (from 0.73 to 16.90  $\text{mmol C m}^{-2} \text{d}^{-1}$ ) barely amounted to 1.1–10.6% of what was produced. It is noteworthy that the range of these percentages was wider in mature waters (from 15 to 39 days). Likewise, the potential contribution of the excreted nitrogen (global average = 0.97  $\text{mmol NH}_4^+ \text{m}^{-2} \text{d}^{-1}$ ) did not exceed more than the  $4.8 \pm 2.3\%$  of the primary producers' requirements. This percentage remained fairly constant irrespective of the system productivity, although zooplankton seemed to fulfill more of the phytoplankton demands in aged waters (Table 3). Overall, the relationship between respiration and  $\text{NH}_4^+$  excretion (O/N ratios) showed higher values in the transition area (from 12 to 20); then, they decreased towards the open ocean to a range of 5 to 13. This means that zooplankton metabolism relied on more protein offshore.

## 4. Discussion

### 4.1. Zooplankton biomass and community structure

The signature of several water masses such as the South Atlantic Central Water (SACW), the East South Atlantic Central Water (ESACW) and the cold filament intrusions from the fresh upwelled waters coexisted in the northern Namibian cell during the study. This coincides with previous findings of Boyd et al. (1987) in the same area. As a result, zooplankton biomass was not distributed uniformly throughout the transect (Fig. 2), but displayed strong temporal and spatial gradients caused by the physical forcing. For instance, the upwelling of deep waters rapidly disrupts the structure of the resident biota, and generates an ecological succession in the aging advected waters. In our study, mature waters rich in nutrients predominated at the end of August over most of the transect, and promoted the enhancement of phytoplankton (Hansen et al., 2014) and eventually of zooplankton, just as the model of Vinogradov et al. (1972) predicted. At this time, zooplankton biomass reached peaks of 65  $\text{mg DM m}^{-3}$  in the upper 200 m of the transition area, which agreed with the values reported in Postel (1995) and Postel et al. (2007) in the upwelled waters north of Walvis Bay, but not with the estimates of zooplankton standing stock recorded in quiescent periods (Olivar and Barangé, 1990; Verheye and Hutchings, 1988). The latter research sampled the northern Benguela during the austral autumn, when the upwelling activity is the most sluggish, resulting in a mean biomass of only 26  $\text{mg DM m}^{-3}$  for the entire

shelf area. This value falls in the range observed in other less productive upwelling systems (Bode et al., 2005; Hernández-León et al., 2002). Here, similar values were measured in September, when filaments were not strongly influencing the transect and thereby, the less productive aged waters dominated in the study area. In general, the low zooplankton biomass found in the newly upwelled waters, increased as it moved seaward to a maximum over the shelf-break. This coincided with the offshore edge of the chlorophyll maxima. Further offshore, the zooplankton biomass decreased dramatically. Such a pattern is in accordance with the spatial trend described in Shannon and Pillar (1986) and Olivar and Barangé (1990). One exception, however, was found in the surface waters 380 km from the coast (NAM023) in mid September (Fig. 4). The extraordinarily high concentration of large organisms (>1000  $\mu\text{m}$ ) at this oceanic station (70  $\text{mg DM m}^{-3}$ ) was explained by the introduction of SACW waters via the filament (see Fig. 6e in Mohrholz et al., 2014). This water still maintained some of its original properties. Accordingly, a successional development in this water mass resulted in a mature plankton community (sensu Vinogradov and Shushkina, 1978) dominated by predatory zooplankton in a low chlorophyll environment.

Overall, the zooplankton correlated with the diatom distribution (Fig. 11), which argues for a “bottom-up” control over the trophic chain as usually occurs in productive ecosystems (Cury and Shannon, 2004). The dominance of chain-forming diatoms in the transition area might entail, however, a food particle size limitation to the microzooplankton (100–200  $\mu\text{m}$ ), whose diet relies primarily on both individual phytoplanktonic cells and small microheterotrophs (Irigoién, 2005). Accordingly, their contribution to the total biomass dropped at the shelf edge (Table 1). Unfortunately, the coarse taxonomic resolution (Fig. 5) constrains our discussion of how the biological forcing, as well as the highly advective environment, disrupted the zooplankton assemblages. In general, the numerical prevalence of copepods that we observed (Fig. 5) concurs with investigations of Timonin (1997) and Loick et al. (2005) for the Benguela ecosystem. However, in our study the pelagic copepods peaked near the coast (6751  $\text{ind m}^{-3}$ ), contrary to the previous findings of maximum densities developing at the outer shelf resulting from advection by Ekman transport (Verheye et al., 1992). Indeed, this offshore transport via filaments together with the inshore upwelling cells, may explain the oceanic occurrence of organisms normally common in neritic waters such as chaetognaths (Gibbons et al., 1992), tintinnids (Dolan et al., 2012) and the benthic harpacticoids that we have documented. Still, other processes such as biological competition may be controlling the pelagic copepod population. With a plentiful food supply, salps can take immediate advantage of their high filtering rates and rapid growth (Alldredge and Madin, 1982), so swarms of these tunicates could easily exclude other planktonic grazers over the shelf-break. Thus, the spatial pattern of

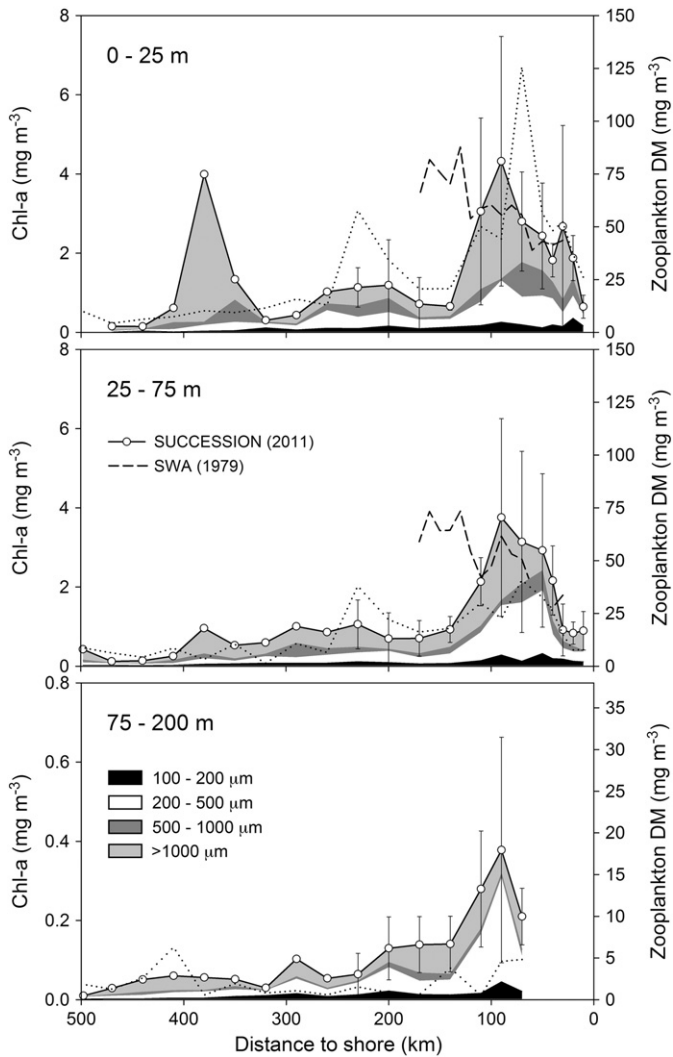


**Fig. 4.** Mean zooplankton biomass at different depth levels with the contribution of each size fraction. Dotted line stands for the chlorophyll-a concentration. Zooplankton biomass data for the SUCCESION cruise are compared (top two panels) with data from the same transect made 32 years before (1979), during the Southwest Atlantic cruise (SWA). No data are shown for the shallow stations along the first 70 km in the bottom panel. Note that the scale for both chlorophyll-a and zooplankton is smaller in the 75–200 m layer. Error bars indicate the 95% C. L., but not for the data seaward of 230 km where only one measurement was made.

zooplankton from the Benguela upwelling seems to be determined in the short-term not only by the complex interplay between mesoscale structures, as the satellite images show, but also by the interspecific relationships linked to the successional development of the water masses.

**4.2. Body composition and stable isotopes in zooplankton**

The data on elemental composition (Table 1) are comparable to DM, carbon and nitrogen content reported for the zooplankton community from the NW Spanish upwelling (Bode et al., 1998). Differences between the three zones were not marked, although a shift in both nutritional source and zooplankton assemblages might explain a slightly higher carbon and nitrogen contribution to the total mass in the transition area. Nonetheless, low carbon content (ranging from 11 to 33% of DM) in comparison to that measured in polar regions (e.g., from 23.5 to 61.0% in Ikeda and Skjoldal, 1989) suggests minor lipid storage by

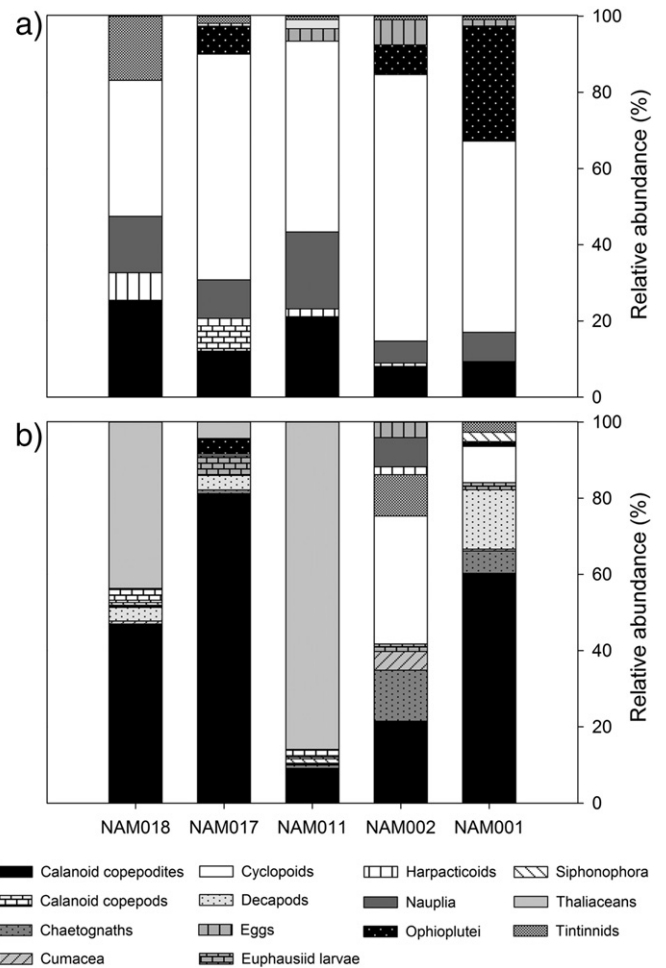


**Fig. 5.** Relative abundances of the taxa which contributed to more than 2% of the zooplankton community abundance in both the 100–500 μm (a) and the >500 μm (b) size classes. Only the upper 25 m of the water-column was considered.

the zooplankton in Benguela. In fact, protein is often the dominant metabolic reserve in areas with abundant and constant food supply (Postel et al., 2000). Likewise, atomic C/N ratios were in a range consistent with those found in several groups of mesozooplankton from the northern Benguela (Schukat et al., 2014), and in marine crustaceans in general (Bode et al., 1998). The larger values in the C/N relationship at the

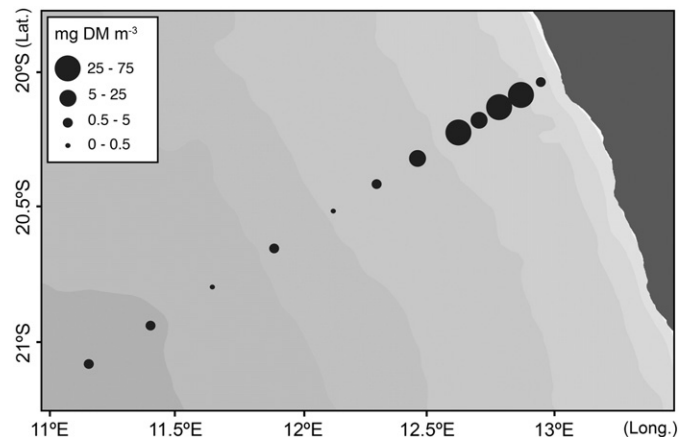


**Fig. 6.** Cross-shelf distribution of jellyfish biomass in the upper 200 m of the water-column, except for the five near-shore stations where the bottom depth was shallower.



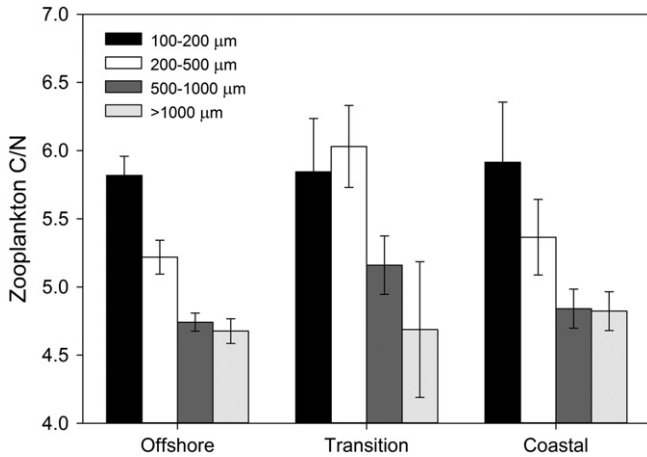


Fig. 7. Averaged atomic C/N ratios for each size fraction in the different zones. Error bars indicate the 95% C. L.

transition zone, however, may reflect a shift in the zooplankton diet (Fig. 7). This enhancement, jointly with lower specific-GDH activities (Table 2), would result in reduced  $\text{NH}_4^+$  excretion rates per unit of biomass in the transition waters (Anderson, 1992). Furthermore, C/N ratios resembled the trend set by the O/N ratios (see Table 3), which provide an indicator of the metabolic substrate oxidized for energy. Depending on the amino-acid and the fatty acid involved in the catabolic pathways, the O/N ratio can theoretically range from 3 to infinity (Mayzaud and Conover, 1988). Accordingly, pure protein catabolism is assumed to yield O/N ratios below 13, while a value of around 24 indicates a reliance on both protein and lipids. In our study, offshore, outside of the filament, the O/N ratios were characteristically between 4 and 6, indicating protein-dominated catabolism. This was likely caused by higher indices of carnivory within this area. On the contrary, at the transition zone the O/N ranged between 12 and 20, which would correspond to a more lipid-rich diet.

Additional ecological understanding is achieved through a study of the zooplankton isotopic composition, since the stable isotopes constitute a useful tool to describe the structure of the food web and nutrient dynamics of a given ecosystem. Thus,  $\delta^{15}\text{N}$  sheds light on the trophic position of organisms as well as on the contribution of isotopically distinct nitrogen sources entering the base of the food chain (Montoya, 2008).  $\delta^{13}\text{C}$  provides insight into the character of the zooplankton carbon source (Koppelman et al., 2009). Here we use both isotopes in order to determine potential changes in dietary relationships in the study area. The significance in the spatial variability in  $\delta^{13}\text{C}$  that we observed

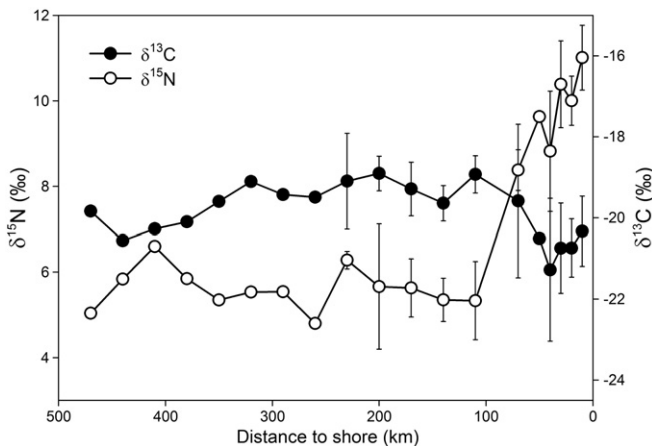


Fig. 8. Spatial variation of averaged zooplankton  $\delta^{15}\text{N}$  and  $\delta^{13}\text{C}$  values along the transect. Note that each value in the first 230 km comes from the average of the four sections. Error bars indicate the 95% C. L.

was likely caused by changes in food resources from the diverse water masses found along the transect (Fig. 8). For instance, zooplankton with small lipid reserves would explain lower  $\delta^{13}\text{C}$  at the inner shelf (Saupe et al., 1989). Preying more on diatoms, which are enriched in  $^{13}\text{C}$  compared to the small flagellates (Fry and Wainright, 1991), would lead to less negative zooplankton- $\delta^{13}\text{C}$  values in transition waters. On the other hand, the differences in  $\delta^{15}\text{N}$  signatures were remarkably greater than the corresponding differences in the  $\delta^{13}\text{C}$  signatures. This likely originated in the source of the nitrogen utilized by phytoplankton rather than in species succession processes, since the same trend was followed by all the size fractions. Thus, upwelled nitrate near the coast is expected to be enriched in  $^{15}\text{N}$  through bacterial remineralization in deep waters. This resulted in a progressive phytoplankton enrichment in  $^{15}\text{N}$  as the primary producers removed dissolved nitrate over the shelf waters (Bode and Álvarez-Ossorio, 2004; O'Reilly et al., 2002). Farther offshore,  $\delta^{15}\text{N}$ -depleted nitrogen-species, such as  $\text{N}_2$  fixed by diazotrophs or  $\text{NH}_4^+$  excreted by heterotrophs, could become dominant in supporting the primary production and therefore, lower  $\delta^{15}\text{N}$  signatures would be propagated into the other components of the trophic chain. Differences in the number of intermediary trophic levels which are channeling the mass transfer through the food web could also explain such a variability, but isotope reference values for phytoplankton would be necessary for confirmation.

#### 4.3. Zooplankton metabolism

In seeking an understanding of the carbon balance it is important to know whether the heterotrophs consume all the primary productivity or whether there is some fixed carbon left over to be exported to the bottom (Ducklow and Doney, 2013). This will depend on the level of primary productivity which will be limited by nitrogen, among other elements. In this scenario, zooplankton metabolism impacts both carbon and nitrogen cycles, with environment, season and taxonomy modulating its biogeochemical role. Compared to shelf waters of other upwelling case studies where zooplankton respiration and  $\text{NH}_4^+$  excretion in the upper 200 m varied from 7.5 to 103.1  $\mu\text{mol O}_2 \text{ m}^{-3} \text{ d}^{-1}$  and from 0.2 to 5.4  $\mu\text{mol NH}_4^+ \text{ m}^{-3} \text{ d}^{-1}$ , respectively (Hernández-León et al., 2002; Isla and Anadón, 2004; Packard et al., 1974; Pérez-Aragón et al., 2011), here zooplankton consumed on average more oxygen (112.4  $\mu\text{mol O}_2 \text{ m}^{-3} \text{ d}^{-1}$ ) and released more  $\text{NH}_4^+$  (10.3  $\mu\text{mol NH}_4^+ \text{ m}^{-3} \text{ d}^{-1}$ ). In spite of this elevated respiration and  $\text{NH}_4^+$  excretion, when compared to the net primary productivity (NPP), the relative values of these two processes were consistent with those measured in NW Africa (Packard, 1979) and in Benguela (Chapman et al., 1994).

The respiratory carbon demand of zooplankton averaged  $7.1 \pm 4.7 \text{ mmol C m}^{-2} \text{ d}^{-1}$  in the whole transect (Table 3). According to the energy budget approach given in Ikeda and Motoda (1978), the ingestion rate can be derived from the respiration by a factor of 2.5. This means that the zooplankton would remove between 6.0 and 29.5  $\text{mmol C m}^{-2} \text{ d}^{-1}$  in the upper 75 m of the water-column, i.e., about 14% of mean daily (net) production if we assume major herbivory and an assimilatory efficiency of 70% (Kjørboe et al., 1985). These estimates are slightly higher than the average copepod consumption rates reported by Schukat et al. (2013) for the northern Benguela (1.8–6.5  $\text{mmol C m}^{-2} \text{ d}^{-1}$ ). Even though Hernández-León and Ikeda (2005) calculated a mesozooplankton carbon demand ranging from 34 to 63% of the global primary productivity, the percentage drops more than three times in eutrophic ecosystems (Calbet, 2001), which encompasses our approximations. It is known that microheterotrophs' grazing often accounts for most of the phytoplankton production, but will these organisms be able to consume the remaining carbon in such a productive system? Parallel research with bacteria during the same cruise (Bergen et al., in prep.) calculated that a consumption of around 29% of the net production was necessary to sustain their metabolic carbon requirements in the upper 75 m (43  $\text{mmol C m}^{-2} \text{ d}^{-1}$ ). In addition, estimations of Chapman et al. (1994) suggested that



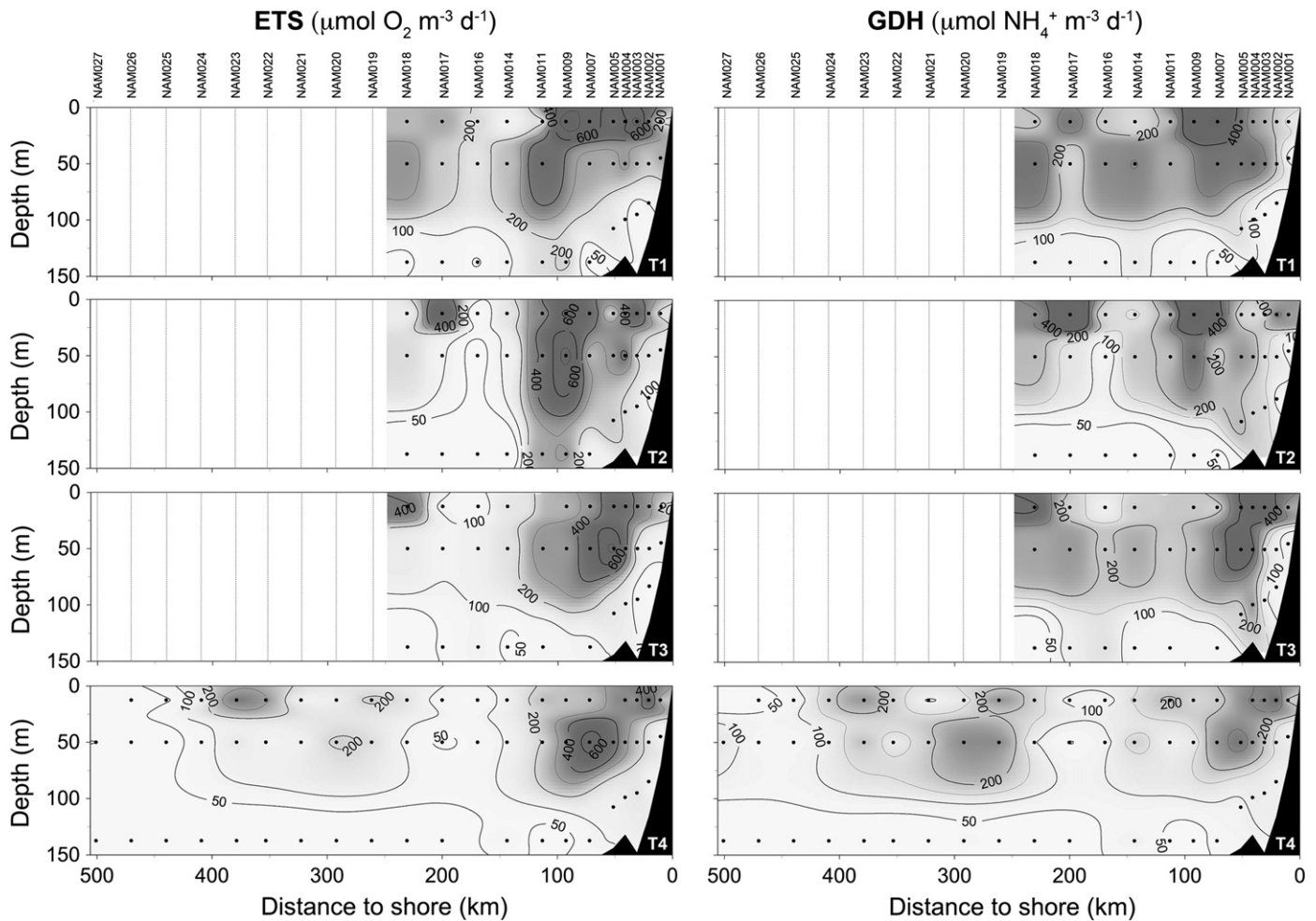


**Fig. 9.** Depth-profiles of zooplankton ETS activities ( $\mu\text{mol O}_2 \text{ m}^{-3} \text{ d}^{-1}$ ) and GDH activities ( $\mu\text{mol NH}_4^+ \text{ m}^{-3} \text{ d}^{-1}$ ) for each transect. Sampling dates in 2011 were as follows: 27 Aug–30 Aug (T1), 31 Aug–02 Sep (T2), 08 Sep–10 Sep (T3) and 11 Sep–15 Sep (T4). ODV software was used to generate interpolated values using the weighted averaged gridding method option.

microplankton would double the carbon losses attributable to zooplankton (i.e., ~28% of the NPP in our case study). Considering the top predators and large gelatinous zooplankton as minor sinks for phytoplankton biomass, it seems reasonable to presume that the system was autotrophic during the active upwelling season. In other words, there was a surplus of net production to be exported. In support of this, estimates by Osma et al. (2014) revealed that an average of about 23% of the NPP was either respired in the water column below 75 m or deposited in the sediments. Some of the remaining NPP was likely exported by the filament towards the open ocean.

The contribution of zooplankton  $\text{NH}_4^+$  excretion to the phytoplankton productivity (Table 3) was also limited (0.5–11.3%). Although a secondary role might be expected for remineralization in areas with large inputs of new nitrogen, there is no obvious pattern about the importance of zooplankton in fueling the primary productivity throughout different ecosystems (Bronk and Steinberg, 2008). Here, the zooplankton did not seem to be a key component of the total  $\text{NH}_4^+$  regeneration via excretion processes. Our results were comparable with the

mesozooplankton regeneration in the upwelling off NW Spain (Bode et al., 2004; Isla et al., 2004). Accordingly, dissolved  $\text{NH}_4^+$  displayed a weak correlation with zooplankton distribution (Fig. 11), although some caution about this interpretation is needed as the  $\text{NH}_4^+$  has a very rapid turnover. In fact, remineralized nitrogen (Benavides et al., 2014) and phosphorus (Nausch and Nausch, 2014) were found necessary to support the large phytoplankton biomass at 20°S. This may reveal a major remineralization pathway through microheterotrophs as Probyn (1987) found for the southern Benguela. Despite the dynamics of zooplankton metabolism in both the time and space domain, we conclude that it had little impact on the NPP in all the different productivity regimes within the Namibian system.

On a physiological basis, the indices of metabolism did not sharply respond to the patterns of chlorophyll-a and productivity. While phytoplankton biomass declined in the transition area, likely due to the grazing pressure and nutrient depletion, high values of specific-ETS activities remained relatively constant from the rich upwelled waters to the oceanic ones (Table 2). Longer life cycles allow zooplankton to

**Table 2**  
Mean values ( $\pm$ SD) of biomass-specific ETS and GDH of size-fractionated zooplankton in coastal (C), transition (T) and offshore (O) stations, averaged over the 200 m water-column.

Size ( $\mu\text{m}$ )	Specific ETS ( $\mu\text{mol O}_2 \text{ mg protein}^{-1} \text{ h}^{-1}$ )			Specific GDH ( $\mu\text{mol NH}_4^+ \text{ mg protein}^{-1} \text{ h}^{-1}$ )		
	C	T	O	C	T	O
100–200	$1.95 \pm 0.65$	$1.98 \pm 0.52$	$2.07 \pm 0.45$	$2.99 \pm 0.87$	$1.16 \pm 0.74$	$2.68 \pm 1.16$
200–500	$2.36 \pm 0.66$	$2.23 \pm 0.59$	$2.46 \pm 0.46$	$2.88 \pm 1.00$	$1.58 \pm 0.79$	$3.77 \pm 0.87$
500–1000	$2.96 \pm 1.14$	$2.12 \pm 0.60$	$2.61 \pm 0.74$	$2.63 \pm 1.01$	$2.25 \pm 1.02$	$3.41 \pm 0.82$
>1000	$2.72 \pm 0.79$	$1.28 \pm 0.39$	$1.66 \pm 0.60$	$1.15 \pm 0.61$	$1.15 \pm 0.57$	$2.09 \pm 0.81$

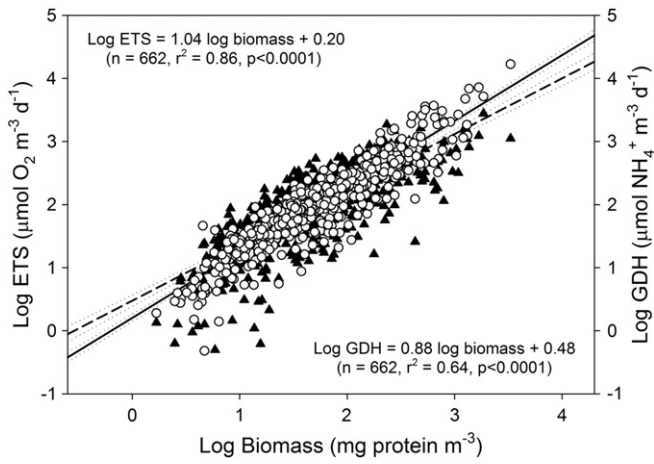


**Fig. 10.** Log-transformed ETS activities (open dots and solid line) and GDH activities (black symbols and dashed line) versus Log-transformed protein mass. Dotted lines limit the 95% confident interval for each regression line.

reside longer in the water-column than the phytoplankton, so they are more intensely subjected to both advection and active transport seaward. During this process, the zooplankton diet shifts gradually into omnivory (Hernández-León et al., 2002), which would sustain a highly active metabolism even offshore. Indeed, more carnivory would explain the decrease in zooplankton biomass and a more protein-based metabolism (as denoted by lower O/N ratios) towards the ocean. In contrast, specific-GDH activities fell in the highly productive transition waters, similar to the findings of Hernández-León et al. (2001) in Canary Islands' waters. Those authors showed negative correlations between GDH and both zooplankton gut content and chlorophyll-a. In fact, GDH activity not only depends on the intracellular substrate availability, but also on the energy charge of the organisms. As the guanosine-5-triphosphate (GTP) levels increase in response to the nutrient-sufficient metabolic states, GDH should be inhibited and, rather than being deaminated, amino acids such as glutamate could be used for growth and protein biosynthesis (Bidigare and King, 1981). Thus, the enhanced O/N ratios over the shelf-break implied a decrease in protein catabolism. Independently of these internal adjustments in

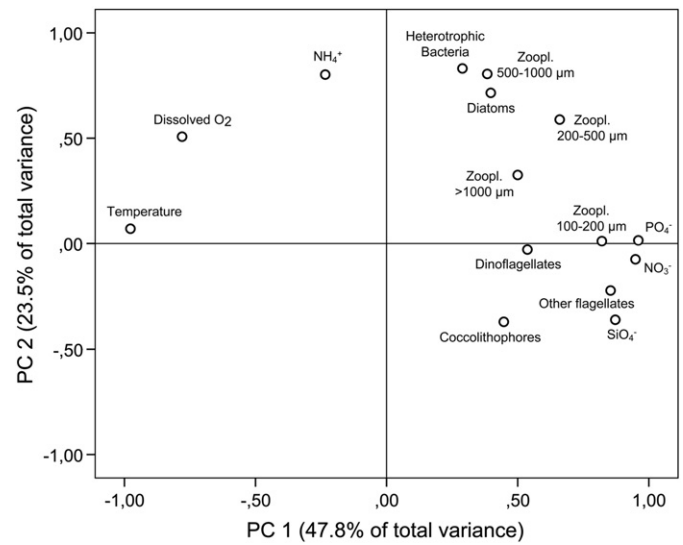


**Fig. 11.** Correlation matrix-based principal component analysis plotted according to the hydrographic characteristics (PC 1) and the occurrence of different biological communities (PC 2). Both axes together explained 71.3% of the total variance. Chemical variables were given in  $\mu\text{M}$  units, while the biological ones were correlated in terms of biomass ( $\text{mg C m}^{-3}$ ). Non-normal data sets were previously normalized through the  $\log(x + 1)$  transformation.

zooplankton biochemistry, both enzymatic indices showed good correlations with biomass, reflecting their constitutive nature as permanent components of living cells. Scaling exponents of 1.04 and 0.88 (Fig. 10) revealed nearly isometric relationships between the potential respiration or  $\text{NH}_4^+$  excretion and protein-biomass, which appears to be a common feature in the metabolism of pelagic organisms (Glazier, 2006). This means that both ETS and GDH activities covary linearly with biomass. However, short-term fluctuations in the environmental conditions might force the physiology to diverge from biomass more rapidly than do the potential rates, resulting in different scaling exponents. This would impact both R/ETS and GDH/ $\text{NH}_4^+$  ratios (Berges et al., 1993; Fernández-Urruzola et al., 2011), but its influence would not be great enough to deter the use of these enzymes as ecological indices.

**Table 3**

Averaged ( $\pm$  SD) net primary production (NPP) for each station, and the respiration and  $\text{NH}_4^+$  excretion of zooplankton in the upper 75 m of the water-column. The resultant O/N ratios as well as the range of NPP (%) both respired and regenerated by zooplankton are also presented. Pseudo-age stands for the estimated age of the waters (mean  $\pm$  SD), as detailed in Mohrholz et al. (this volume). Note that no SDs are given from NAM019 to NAM027 as these stations were sampled just once. A dash indicates data not determined.

Station	Pseudo-age (d)	NPP ( $\text{mmol C m}^{-2} \text{d}^{-1}$ )	Respiration ( $\text{mmol C m}^{-2} \text{d}^{-1}$ )	% NPP <sub>Resp.</sub>	$\text{NH}_4^+$ excretion ( $\text{mmol NH}_4^+ \text{m}^{-2} \text{d}^{-1}$ )	% NPP <sub>Regen.</sub>	O/N
NAM001	5.3 $\pm$ 2.9	64.4 $\pm$ 24.2	4.60 $\pm$ 1.81	6.9–7.2	0.45 $\pm$ 0.09	3.7–5.5	11.0 $\pm$ 8.7
NAM002	7.3 $\pm$ 3.4	123.0 $\pm$ 14.3	7.24 $\pm$ 2.41	4.4–7.0	1.01 $\pm$ 0.11	5.0–5.1	10.3 $\pm$ 7.6
NAM003	11.0 $\pm$ 1.8	123.7 $\pm$ 50.8	10.19 $\pm$ 6.14	5.6–9.4	0.95 $\pm$ 0.34	4.5–5.1	10.3 $\pm$ 7.4
NAM004	15.5 $\pm$ 4.2	169.7 $\pm$ 37.3	12.76 $\pm$ 2.55	7.4–7.7	1.60 $\pm$ 0.60	4.6–6.5	12.2 $\pm$ 10.4
NAM005	23.3 $\pm$ 10.7	184.2 $\pm$ 50.4	14.32 $\pm$ 10.54	2.8–10.6	1.74 $\pm$ 0.74	4.6–6.4	12.1 $\pm$ 7.2
NAM007	31.5 $\pm$ 16.1	215.2 $\pm$ 49.0	14.22 $\pm$ 4.87	5.6–7.2	1.44 $\pm$ 0.58	3.2–4.7	14.5 $\pm$ 11.1
NAM009	38.9 $\pm$ 10.8	210.8 $\pm$ 66.7	16.90 $\pm$ 11.30	3.9–10.2	1.55 $\pm$ 1.44	0.5–6.6	19.9 $\pm$ 13.2
NAM011	70.1 $\pm$ 18.6	196.4 $\pm$ 27.1	9.64 $\pm$ 2.79	4.0–5.6	0.82 $\pm$ 0.19	2.3–2.8	15.1 $\pm$ 10.8
NAM014	78.2 $\pm$ 8.0	109.4 $\pm$ 27.0	4.64 $\pm$ 1.29	4.1–4.3	0.98 $\pm$ 0.14	5.0–6.2	5.8 $\pm$ 2.0
NAM016	74.9 $\pm$ 11.2	113.7 $\pm$ 16.0	3.23 $\pm$ 2.18	1.1–4.2	0.79 $\pm$ 0.35	2.7–5.4	4.5 $\pm$ 2.5
NAM017	62.5 $\pm$ 22.9	154.1 $\pm$ 53.7	4.65 $\pm$ 3.44	1.2–3.9	0.93 $\pm$ 0.56	2.2–4.4	6.6 $\pm$ 3.8
NAM018	62.1 $\pm$ 15.9	110.0 $\pm$ 39.4	6.25 $\pm$ 2.56	5.2–5.9	1.06 $\pm$ 0.43	5.4–6.1	7.1 $\pm$ 2.7
NAM019	68.9	86.3	7.06	8.2	1.60	11.3	5.3
NAM020	68.7	111.0	6.39	5.8	1.12	6.2	6.3
NAM021	67.4	94.1	2.27	2.4	0.61	4.0	4.8
NAM022	82.8	106.1	5.20	4.9	0.47	2.7	12.7
NAM023	85.6	87.7	8.99	10.3	1.25	8.7	8.6
NAM024	86.8	74.1	1.97	2.7	0.59	4.9	4.5
NAM025	100.3	68.1	0.77	1.1	0.22	2.0	5.6
NAM026	104.6	72.9	0.73	1.0	0.16	1.3	6.9
NAM027	104.3	87.8	–	–	–	–	–

## 5. Conclusions

The distribution of zooplankton biomass as well as the impact of its metabolism on the northern Namibian phytoplankton community during active upwelling have been described here. Our results are in broad agreement with previous findings from this system. Zooplankton biomass and metabolic rates fluctuated highly with the upwelling filaments, but their maxima were characteristically observed over the outer shelf. Thus, there was a horizontal zonation determined by the hydrographic and hydrochemical conditions. The pelagic copepods dominated the zooplankton in all parts of the transect. Nevertheless, the structure of the community was strongly altered by salp blooms over the shelf-break. On average, the elemental composition of zooplankton indicated low lipid storage in the study area. This was more noticeable in neritic waters, where plankton with lower  $\delta^{13}\text{C}$  such as flagellates constituted the main carbon resource for zooplankton. In addition, the spatial pattern of zooplankton- $\delta^{15}\text{N}$  in the aging advected waters revealed a progressive substitution of the nitrogen-species that sustained the biological production.

The zooplankton respiration and  $\text{NH}_4^+$  excretion rates in the highly productive waters of the northern Benguela exceeded those measured in other upwelling systems. Still, this respiration consumed just a small proportion of the daily primary production (1.1–10.6%). Accordingly, the northern Benguela ecosystem acted as an autotrophic system during the intense wind-forcing season. High protein-specific respiration rates over the entire transect suggested an enhancement in omnivory over herbivory in the low-chlorophyll offshore area. This also explains the decrease in zooplankton biomass and the increase in protein-catabolism towards the open ocean. Parallel with the respiration, zooplankton  $\text{NH}_4^+$  excretion only contributed 0.5 to 11.3% of primary production's nitrogen requirements. Therefore, most of the organic matter produced in these Namibian waters should be recycled through the microbial food web.

## Acknowledgments

We wish to thank the crew of the RV Maria S. Merian for their assistance during the cruise, and the researchers involved in collecting the samples. We are also grateful to I. Martínez for the protein determinations, to A. Herrera for her collaboration in ETS measurements, to I. Liskow for the isotopic analyses as well as to S. Rubin for the taxonomic characterization. Furthermore, N. Wasmund kindly lent us his  $^{14}\text{C}$  data. Comments from anonymous referees also contributed in improving the manuscript. This work was funded by the German Research Foundation (DFG) cruise support and by the BIOMBA project (CTM2012-32729/MAR). The latter was granted to M. Gómez by the Spanish Economy and Competitiveness Ministry. I. Fernández-Urruzola and N. Osma received financial support from the Formation and Perfection of the Researcher Personal Program from the Basque Government. T.T. Packard was partially supported by a grant from the Leibniz Institute for Baltic Sea Research.

## References

Allredge, A.L., Madin, L.P., 1982. Pelagic tunicates: unique herbivores in the marine plankton. *Bioscience* 32 (8), 655–663.

Anderson, T.R., 1992. Modelling the influence of food C:N ratio, and respiration on growth and nitrogen excretion in marine zooplankton and bacteria. *J. Plankton Res.* 14 (12), 1645–1671.

Banše, K., 1977. Determining the carbon-to-chlorophyll ratio of natural phytoplankton. *Mar. Biol.* 41 (3), 199–212.

Benavides, M., Santana, Y., Wasmund, N., Aristegui, J., 2014. Microbial uptake and regeneration of inorganic nitrogen off the coastal Namibian upwelling system. *J. Mar. Syst.* 140, 51–57.

Berges, J.A., Roff, J.C., Ballantyne, J.S., 1993. Enzymatic indices of respiration and ammonia excretion: relationships to body size and food levels. *J. Plankton Res.* 15 (2), 239–254.

Bigdare, R.R., 1983. Nitrogen excretion in marine zooplankton. In: Carpenter, E.J., Capone, D.G. (Eds.), *Nitrogen in the Marine Environment*. Academic Press, New York, pp. 385–409.

Bigdare, R.R., King, F.D., 1981. The measurement of glutamate dehydrogenase activity in *Praunus flexuosus* and its role in the regulation of ammonium excretion. *Comp. Biochem. Physiol.* 70 (B), 409–413.

Bode, A., Álvarez-Ossorio, M.T., 2004. Taxonomic versus trophic structure of mesozooplankton: a seasonal study of species succession and stable carbon and nitrogen isotopes in a coastal upwelling ecosystem. *ICES J. Mar. Sci.* 61 (4), 563–571.

Bode, A., Álvarez-Ossorio, M.T., González, N., 1998. Estimations of mesozooplankton biomass in a coastal upwelling area off NW Spain. *J. Plankton Res.* 20 (5), 1005–1014.

Bode, A., Barquero, S., González, N., Álvarez-Ossorio, M.T., Varela, M., 2004. Contribution of heterotrophic plankton to nitrogen regeneration in the upwelling ecosystem of A Coruña (NW Spain). *J. Plankton Res.* 26 (1), 11–28.

Bode, A., Álvarez-Ossorio, M.T., González, N., Lorenzo, J., Rodríguez, C., Varela, M., Varela, M.M., 2005. Seasonal variability of plankton blooms in the Ria de Ferrol (NW Spain): II. Plankton abundance, composition and biomass. *Estuar. Coast. Shelf Sci.* 63 (1–2), 285–300.

Bode, M., Schukat, A., Hagen, W., Auel, H., 2013. Predicting metabolic rates of calanoid copepods. *J. Exp. Mar. Biol. Ecol.* 444, 1–7.

Boltovskoy, D., 1999. *South Atlantic Zooplankton*, vol. 1. Backhuys, Leiden (1075 pp.).

Boyd, A.J., Salat, J., Masó, M., 1987. The seasonal intrusion of relatively saline water on the shelf off northern and central Namibia. *Afr. J. Mar. Sci.* 5 (1), 107–120.

Boyer, D., Cole, J., Bartholomae, C., 2000. Southwestern Africa: Northern Benguela current region. *Mar. Pollut. Bull.* 41 (1–6), 123–140.

Bronk, D.A., Steinberg, D.K., 2008. Nitrogen regeneration. In: Capone, D.G., Bronk, D.A., Mulholland, M.R., Carpenter, E.J. (Eds.), *Nitrogen in the Marine Environment*. Academic Press, London, pp. 385–467.

Brown, P.C., Painting, S.J., Cochrane, K.L., 1991. Estimates of phytoplankton and bacterial biomass and production in the northern and southern Benguela ecosystems. *Afr. J. Mar. Sci.* 11 (1), 537–564.

Calbet, A., 2001. Mesozooplankton grazing effect on primary production: a global comparative analysis in marine ecosystems. *Limnol. Oceanogr.* 46 (7), 1824–1830.

Chapman, P., Mitchell-Innes, B.A., Walker, R., 1994. Microplankton ETS measurements as a means of assessing respiration in the Benguela ecosystem. *Afr. J. Mar. Sci.* 14, 297–312.

Cury, P., Shannon, L., 2004. Regime shifts in upwelling ecosystems: observed changes and possible mechanisms in the northern and southern Benguela. *Prog. Oceanogr.* 60, 223–243.

del Giorgio, P.A., 1992. The relationship between ETS (electron transport system) activity and oxygen consumption in lake plankton: a cross-system calibration. *J. Plankton Res.* 14 (12), 1723–1741.

Dolan, R.J., Montagnes, D.J.S., Agatha, S., Coats, D.W., Stoecker, D.K., 2012. *The Biology and Ecology of Tintinnid Ciliates: Models for Marine Plankton*, 1st ed. Wiley-Blackwell, Chichester, UK, (296 pp.).

Ducklow, H.W., Doney, S.C., 2013. What is the metabolic state of the oligotrophic ocean? A debate. *Annu. Rev. Mar. Sci.* 5 (1), 525–533.

Dugdale, R.C., Goering, J.J., 1967. Uptake of new and regenerated forms of nitrogen in primary productivity. *Limnol. Oceanogr.* 12, 196–206.

Fernández-Urruzola, I., Packard, T.T., Gómez, M., 2011. GDH activity and ammonium excretion in the marine mysid *Leptomysis lingvura*: effects of age and starvation. *J. Exp. Mar. Biol. Ecol.* 409 (1–2), 21–29.

Fry, B., Wainright, S.C., 1991. Diatom sources of  $^{13}\text{C}$ -rich carbon in marine food webs. *Mar. Ecol. Prog. Ser.* 76, 149–157.

Gaudy, R., Youssara, F., 2003. Variations of zooplankton metabolism and feeding in the frontal area of the Alboran Sea (western Mediterranean) in winter. *Oceanol. Acta* 26 (2), 179–189.

Gibbons, M.J., 1997. An Introduction to the Zooplankton of the Benguela Current Region. Zoology department, University of Western Cape, Cape Town, South Africa, (51 pp.).

Gibbons, M.J., Hutchings, L., 1996. Zooplankton diversity and community structure around southern Africa, with special attention to the Benguela upwelling system. *S. Afr. J. Sci.* 92 (2), 63–77.

Gibbons, M.J., Stuart, V., Verheye, H.M., 1992. Trophic ecology of carnivorous zooplankton in the Benguela. *Afr. J. Mar. Sci.* 12 (1), 421–437.

Glazier, D.S., 2006. The 3/4-Power law is not universal: evolution of isometric, ontogenetic metabolic scaling in pelagic animals. *Bioscience* 56 (4), 325–332.

Hansen, F.C., Cloete, R.R., Verheye, H.M., 2005. Seasonal and spatial variability of dominant copepods along a transect off Walvis Bay (23°S) Namibia. *Afr. J. Mar. Sci.* 27 (1), 55–63.

Hansen, A., Wasmund, N., Ohde, T., 2014. Succession of micro- and nanoplankton groups in ageing upwelled waters off Namibia. *J. Mar. Syst.* 140, 130–137.

Hernández-León, S., Gómez, M., 1996. Factors affecting the respiration/ETS ratio in marine zooplankton. *J. Plankton Res.* 18 (2), 239–255.

Hernández-León, S., Ikeda, T., 2005. A global assessment of mesozooplankton respiration in the ocean. *J. Plankton Res.* 27 (2), 153–158.

Hernández-León, S., Postel, L., Aristegui, J., Gómez, M., Montero, M.F., Torres, S., Almeida, C., Kühner, E., Brenning, U., Hagen, E., 1999. Large-scale and mesoscale distribution of plankton biomass and metabolic activity in the Northeastern Central Atlantic. *J. Oceanogr.* 55, 471–482.

Hernández-León, S., Almeida, C., Gómez, M., Torres, S., Montero, I., Portillo-Hahnefeld, A., 2001. Zooplankton biomass and indices of feeding and metabolism in island-generated eddies around Gran Canaria. *J. Mar. Syst.* 30, 51–66.

Hernández-León, S., Almeida, C., Portillo-Hahnefeld, A., Gómez, M., Rodríguez, J.M., Aristegui, J., 2002. Zooplankton biomass and indices of feeding and metabolism in relation to an upwelling filament off northwest Africa. *J. Mar. Res.* 60, 327–346.

Huenerfage, K., Buchholz, F., 2013. Krill of the northern Benguela Current and the Angola-Benguela frontal zone compared: physiological performance and short-term starvation in *Euphausia hansenii*. *J. Plankton Res.* 35 (2), 337–351.



- Huggett, J., Verheye, H., Escribano, R., Fairweather, T., 2009. Copepod biomass, size composition and production in the Southern Benguela: spatio-temporal patterns of variation and comparison with other eastern boundary upwelling systems. *Prog. Oceanogr.* 83 (1–4), 197–207.
- Hutchings, L., Pillar, S.C., Verheye, H.M., 1991. Estimates of standing stock, production and consumption of meso- and macrozooplankton in the Benguela ecosystem. *Afr. J. Mar. Sci.* 11 (1), 499–512.
- Hutchings, L., van der Lingen, C.D., Shannon, L.J., Crawford, R.J.M., Verheye, H.M.S., Bartholomae, C.H., van der Plas, A.K., Louw, D., Kreiner, A., Ostrowski, M., Fidel, Q., Barlow, R.G., Lamont, T., Coetzee, J., Shillington, F., Veitch, J., Currie, J.C., Monteiro, P.M.S., 2009. The Benguela Current: an ecosystem of four components. *Prog. Oceanogr.* 83 (1–4), 15–32.
- ICES, 2001. ICES Identification Leaflets for Plankton, 1939–2001. International Council for the Exploration of the Sea, pp. 1–187.
- Ikeda, T., Motoda, S., 1978. Estimated zooplankton production and their ammonia excretion in the Kuroshio and adjacent seas. *Fish. Bull.* 76 (2), 357–367.
- Ikeda, T., Skjoldal, H.R., 1989. Metabolism and elemental composition of zooplankton from the Barents Sea during early Arctic summer. *Mar. Biol.* 100, 173–183.
- Irigoin, X., 2005. Phytoplankton blooms: a “loophole” in microzooplankton grazing impact? *J. Plankton Res.* 27 (4), 313–321.
- Isla, J.A., Anadón, R., 2004. Mesozooplankton size-fractionated metabolism and feeding off NW Spain during autumn: effects of a poleward current. *ICES J. Mar. Sci.* 61 (4), 526–534.
- Isla, J.A., Ceballos, S., Anadón, R., 2004. Mesozooplankton metabolism and feeding in the NW Iberian upwelling. *Estuar. Coast. Shelf Sci.* 61 (1), 151–160.
- King, F.D., 1984. Vertical distribution of zooplankton glutamate dehydrogenase in relation to chlorophyll in the vicinity of the Nantucket Shoals. *Mar. Biol.* 79, 249–256.
- King, F.D., Packard, T.T., 1975. Respiration and the activity of the respiratory electron transport system in marine zooplankton. *Limnol. Oceanogr.* 20 (5), 849–854.
- Kjørboe, T., Møhlenberg, F., Hamburger, K., 1985. Bioenergetics of the planktonic copepod *Acartia tonsa*: relation between feeding, egg production and respiration, and composition of specific dynamic action. *Mar. Ecol. Prog. Ser.* 26, 85–97.
- Koppelman, R., Bottger-Schnack, R., Mobius, J., Weikert, H., 2009. Trophic relationships of zooplankton in the eastern Mediterranean based on stable isotope measurements. *J. Plankton Res.* 31 (6), 669–686.
- Loick, N., Ekau, W., Verheye, H.M., 2005. Water-body preferences of dominant calanoid copepod species in the Angola-Benguela frontal zone. *Afr. J. Mar. Sci.* 27 (3), 597–608.
- Lowry, O.H., Rosebrough, N.J., Farr, A.L., Randall, R.J., 1951. Protein measurement with the folin phenol reagent. *J. Biol. Chem.* 193, 265–275.
- Maldonado, F., Packard, T.T., Gómez, M., 2012. Understanding tetrazolium reduction and the importance of substrates in measuring respiratory electron transport activity. *J. Exp. Mar. Biol. Ecol.* 434–435, 110–118.
- Margalef, R., 1982. *Ecología*. Omega, Barcelona, (951 pp.).
- Mayzaud, P., Conover, R.J., 1988.  $\delta^{15}\text{N}$  atomic ratio as a tool to describe zooplankton metabolism. *Mar. Ecol. Prog. Ser.* 45, 289–302.
- Mohrholz, V., Eggert, A., Junkers, T., Nausch, G., Ohde, T., Schmidt, M., 2014. Cross shelf hydrographic and hydrochemical conditions and its short term variability at the northern Benguela during a normal upwelling season. *J. Mar. Syst.* 140, 20–38.
- Møller, L.F., Riisgård, H.U., 2007. Respiration in the scyphozoan jellyfish *Aurelia aurita* and two hydromedusae (*Sarsia tubulosa* and *Aequorea vitrina*): effect of size, temperature and growth. *Mar. Ecol. Prog. Ser.* 330, 149–154.
- Moloney, C.L., 1992. Simulation studies of trophic flows and nutrient cycles in Benguela upwelling foodwebs. *Afr. J. Mar. Sci.* 12 (1), 457–476.
- Montoya, J.P., 2008. Nitrogen stable isotopes in marine environments. In: Capone, D.G., Bronk, D.A., Mulholland, M.R., Carpenter, E.J. (Eds.), *Nitrogen in the Marine Environment*. Academic Press, London, pp. 1277–1302.
- Nausch, M., Nausch, G., 2014. Phosphorus speciation and transformation along transects in the Benguela upwelling region. *J. Mar. Syst.* 140, 39–50.
- Olivar, M.P., Barangé, M., 1990. Zooplankton of the northern Benguela region in a quiescent upwelling period. *J. Plankton Res.* 12 (5), 1023–1044.
- Omori, M., Ikeda, T., 1984. *Methods in Marine Zooplankton Ecology*. John Wiley & Sons, Ltd., New York, (332 pp.).
- O’Reilly, C.M., Hecky, R.E., Cohen, A.S., Plisnier, P.D., 2002. Interpreting stable isotopes in food webs: recognizing the role of time averaging at different trophic levels. *Limnol. Oceanogr.* 47 (1), 306–309.
- Osma, N., Fernández-Urruzola, I., Packard, T.T., Postel, L., Gómez, M., Pollehene, F., 2014. Short-term patterns of vertical particle flux in northern Benguela: a comparison between sinking POC and respiratory carbon consumption. *J. Mar. Syst.* 140, 150–162.
- Owens, T., King, F.D., 1975. The measurement of respiratory electron transport system activity in marine zooplankton. *Mar. Biol.* 30 (1), 27–36.
- Packard, T.T., 1979. Respiration and respiratory electron transport activity in plankton from the Northwest African upwelling area. *J. Mar. Res.* 37 (4), 711–742.
- Packard, T.T., 1985. Oxygen consumption in the ocean: measuring and mapping with enzyme analysis. In: Zirino, A. (Ed.), *Mapping Strategies in Chemical Oceanography*. American Chemical Society, Washington D.C., pp. 177–209.
- Packard, T.T., Harmon, D., Boucher, D., 1974. Respiratory electron transport activity in plankton from upwelled waters. *Tethys* 6 (1–2), 213–222.
- Packard, T.T., Devol, A., King, F.D., 1975. The effect of temperature on the respiratory electron transport system in marine plankton. *Deep-Sea Res.* 22 (4), 237–249.
- Park, Y.C., Carpenter, E.J., Falkowski, P.G., 1986. Ammonium excretion and glutamate dehydrogenase activity of zooplankton in Great South Bay New York. *J. Plankton Res.* 8 (3), 489–503.
- Parsons, T.R., Maita, Y., Lalli, C.M., 1984. *Manual of Chemical and Biological Methods for Seawater Analysis*. Pergamon Press, New York, (173 pp.).
- Pérez-Aragón, M., Fernández, C., Escribano, R., 2011. Nitrogen excretion by mesozooplankton in a coastal upwelling area: seasonal trends and implications for biological production. *J. Exp. Mar. Biol. Ecol.* 406 (1–2), 116–124.
- Postel, L., 1995. Rostock zooplankton studies off West Africa. *Helgoländer Meeresun.* 49, 829–857.
- Postel, L., Fock, H., Hagen, W., Skjoldal, H.R., Huntley, M., 2000. Biomass and abundance. In: Harris, R.P., Wiebe, P.H., Lenz, J., Skjoldal, H.R., Huntley, M. (Eds.), *Zooplankton Methodology Manual*. Academic Press, San Diego, pp. 83–192.
- Postel, L., da Silva, A.J., Mohrholz, V., Lass, H.U., 2007. Zooplankton biomass variability off Angola and Namibia investigated by a lowered ADCP and net sampling. *J. Mar. Syst.* 68 (1–2), 143–166.
- Probyn, T.A., 1987. Ammonium regeneration by microplankton in an upwelling environment. *Mar. Ecol. Prog. Ser.* 37, 53–64.
- Richardson, K., 1991. Comparison of  $^{14}\text{C}$  primary production determinations made by different laboratories. *Mar. Ecol. Prog. Ser.* 72, 189–201.
- Richardson, A.J., Verheye, H.M., 1999. Growth rates of copepods in the southern Benguela upwelling system: the interplay between body size and food. *Limnol. Oceanogr.* 44 (2), 382–392.
- Ricker, W.E., 1973. Linear regressions in fishery research. *J. Fish. Res. Board Can.* 30 (3), 409–434.
- Riedl, R., 1983. *Flora und fauna des mittelmeeeres*. Paul Parey, Hamburg und Berlin, (836 pp.).
- Rutter, W.J., 1967. Protein determination in Embryos. In: Wilt, F.H., Wessels, N.V. (Eds.), *Methods in Developmental Biology*. Academic Press, London, pp. 671–684.
- Saupe, S.M., Schell, D.M., Griffiths, W.B., 1989. Carbon-isotope ratio gradients in western arctic zooplankton. *Mar. Biol.* 103 (4), 427–432.
- Schlüter, L., Havskum, H., 1997. Phytoplankton pigments in relation to carbon content in phytoplankton communities. *Mar. Ecol. Prog. Ser.* 155, 55–65.
- Schukat, A., Teuber, L., Hagen, W., Wasmund, N., Auel, H., 2013. Energetics and carbon budgets of dominant calanoid copepods in the northern Benguela upwelling system. *J. Exp. Mar. Biol. Ecol.* 442, 1–9.
- Schukat, A., Auel, H., Teuber, L., Lahajnar, N., Hagen, W., 2014. Complex trophic interactions of calanoid copepods in the Benguela upwelling system. *J. Sea Res.* 85, 186–196.
- Segel, I.H., 1993. *Enzyme Kinetics. Behaviour and Analysis of Rapid Equilibrium and Steady-State Enzyme Systems*. John Wiley & Sons, Inc., New York, (996 pp.).
- Shannon, L.V., 2001. Benguela Current. In: Steele, J.H., Thorpe, S.A., Turekian, K.K. (Eds.), *Encyclopedia of Ocean Sciences*. Academic Press, Amsterdam, pp. 255–267.
- Shannon, L.V., Nelson, G., 1996. The Benguela: large scale features and processes and system variability. In: Wefer, G., Berger, W.H., Siedler, G., Webb, D.J. (Eds.), *The South Atlantic: Present and Past Circulation*. Springer-Verlag, Heidelberg, pp. 163–210.
- Shannon, L.V., Pillar, S.C., 1986. The Benguela ecosystem part III. Plankton. *Oceanogr. Mar. Biol. Annu. Rev.* 24, 65–170.
- Smetacek, V., Hendrikson, P., 1979. Composition of particulate organic matter in Kiel Bight in relation to phytoplankton succession. *Oceanol. Acta* 2 (3), 287–298.
- Solorzano, L., 1969. Determination of ammonia in natural waters by the phenylhypochlorite method. *Limnol. Oceanogr.* 14 (5), 799–801.
- Timonin, A.G., 1997. Diurnal vertical migrations of zooplankton in the upwelling area off the western coast of South Africa. *Oceanology* 37 (1), 83–88.
- Timonin, A.G., Arashkevich, E.G., Drits, A.V., Semenova, T.N., 1992. Zooplankton dynamics in the northern Benguela ecosystem, with special reference to the copepod *Calanoides carinatus*. *Afr. J. Mar. Sci.* 12 (1), 545–560.
- Trégouboff, G., Rose, M., 1978. *Manuel de planctologie méditerranéenne*. Centre National de la Recherche Scientifique, Paris, (587 pp.).
- Van Guelpen, L., Markle, D.F., Duggan, D.J., 1982. An evaluation of accuracy, precision, and speed of several zooplankton subsampling techniques. *J. Conseil.* 40 (3), 226–236.
- Verheye, H.M., Hutchings, L., 1988. Horizontal and vertical distribution of zooplankton biomass in the southern Benguela, May 1983. *Afr. J. Mar. Sci.* 6 (1), 255–265.
- Verheye, H.M., Hutchings, L., Huggett, J.A., Painting, S.J., 1992. Mesozooplankton dynamics in the Benguela ecosystem, with emphasis on the herbivorous copepods. *Afr. J. Mar. Sci.* 12 (1), 561–584.
- Verheye, H.M., Richardson, A.J., Hutchings, L., Marska, G., Gianakouras, D., 1998. Long-term trends in the abundance and community structure of coastal zooplankton in the southern Benguela system, 1951–1996. *Afr. J. Mar. Sci.* 19 (1), 317–332.
- Verheye, H.M., Rogers, C., Maritz, B., Hashoongo, V., Arendse, L.M., Gianakouras, D., Giddey, C.J., Herbert, V., Jones, S., Kemp, A.D., C. R., 2001. Variability of zooplankton in the region of the Angola-Benguela Front during winter 1999. *S. Afr. J. Sci.* 97, 257–258.
- Vinogradov, M.E., Shushkina, E.A., 1978. Some development patterns of plankton communities in the upwelling areas of the Pacific ocean. *Mar. Biol.* 48, 357–366.
- Vinogradov, M.E., Metschunkin, V.V., Shushkina, E.A., 1972. On mathematical simulation of a pelagic ecosystem in tropical waters of the ocean. *Mar. Biol.* 16, 261–268.